DETECTION OF CAVITATION IN FUEL INJECTOR NOZZLES

David P. Schmidt, Tzay-Fa Su, Kayhan H. Goney, P. V. Farrell, M. L. Corradini
Engine Research Center
University of Wisconsin
Madison, WI 53706

ABSTRACT

An experimental investigation to detect cavitation in the nozzles of working Diesel injectors was conducted. Cavitation behavior of Diesel injectors was characterized by a non-dimensional cavitation parameter and a coefficient of discharge. Transient behavior in Diesel injectors with different needle opening pressures and different numbersof nozzle holes was observed and measured. The behavior of sharp-edged single and multi-hole injector tips was found to be reasonably consistent with established characteristics of cavitating nozzles, as observed in steady-state experiments and as predicted by a one-dimensional model. The measurement of flow through a rounded multi-hole tip was consistent with the known behavior of non-cavitating nozzles.

INTRODUCTION

One important method of reducing emissions in Diesel engines is to improve fuel injector spray breakup, producing smaller and more disperse droplets. The flow inside the fuel injector nozzle is known to have a significant effect on the spray, but researchers have not discovered the exact nature of this effect [1]. Recent investigations have suggested that cavitation occurring within the fuel injector nozzle significantly affects spray breakup [2, 3]. However, much of what we know about cavitating nozzles has come from scaled-up models, with precisely determined geometry. Real fuel injector nozzles may have minute imperfections which can cause significant changes in the flow [4].

This investigation uses an experimental technique to indirectly detect the existence of cavitation in a variety of real injectors. The results of this technique should prove especially interesting in more complicated, multi-hole injectors. This experimental method will be applied to a single hole pump line injector and a multi-hole hydraulic electronic unit injector with sharp and rounded nozzle inlets.

A One-Dimensional Model of Cavitating Nozzles

Cavitation bubbles form because of the very low static pressure that occurs in high speed nozzle flow near a sharp inlet corner. This low static pressure is predicted by incompressible potential flow theory, which indicates that flow around a sharp corner, (e.g. a corner with a zero radius of curvature), will have infinite negative pressure. This physically impossible result is a direct consequence of the constant density restriction. In real injectors the fuel density decreases with decreasing pressure, most likely leading to a change in phase. The sharper the corner and the higher the velocity, the more likely cavitation is to occur.

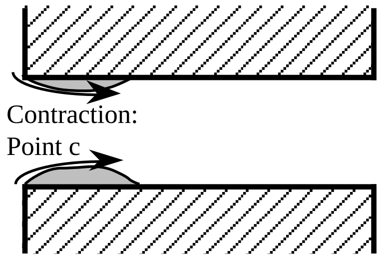

Figure 1. Schematic of nozzle flow

In the case of a sharp inlet, where the flow separates at the corner, the flow experiences a *vena contracta*. A diagram of the sharp entrance flow is shown in Fig. 1. Point 1 would be downstream of the injector needle and yet far enough upstream of the nozzle that the local velocity would be small, such as in the sac of the injector. Point c is downstream of the inlet, where the vena contracta effect is a maximum. In the case of a sufficiently rounded nozzle this point is nonexistent, in which case this analysis may not be useful.

For convenience a ratio between the area at the contraction and the nominal nozzle area, known as the coefficient of contraction, is defined:

$$C_c \equiv \frac{A_c}{A} \tag{1}$$

A_c represents the effective flow area through the contraction and A represents the nominal nozzle area. The value of the contraction coefficient varies with the nozzle geometry and cavitation characteristics. For a very rounded entrance, the flow will not separate and the coefficient of contraction will be unity. For a short nozzle with a sharp entrance, conformal mapping by von Mises predicts a coefficient of contraction of 0.611 [5]. Experimental data seems to suggest that the coefficient of contraction is a constant with respect to Reynolds number, upstream pressure, and downstream pressure [6, 7]. Interestingly, the steady state coefficient of contraction for a sharp entrance seems to be around 0.61 for both cavitating and non-cavitating nozzles, as measured by Numachi [7]. When and how much the contraction area varies is very important and not well known. At increasingly high injection pressures the vapor region which bounds the contraction has been observed to elongate, apparently without further constricting the flow [8].

Another relevant integral property of the flow is the coefficient of discharge, C_d. The coefficient of discharge represents the efficiency of the nozzle between points 1 and 2 and thus is a measure of whatever losses occur in the nozzle The definition of the coefficient of discharge is:

$$C_d \equiv \frac{\dot{m}}{A\sqrt{2\rho\left(P_1 - P_2\right)}} \tag{2}$$

In order to get closure for the one-dimensional model, an important assumption is made. We assume that the pressure at the point of contraction in a cavitating nozzle is equal to the vapor pressure, P_v. In this simplified view of the nozzle, all the losses are assumed to occur between c and 2. The mass flow rate behaves quite peculiarly under these assumptions. If the contraction pressure, P_c, is fixed at the vapor pressure, P_v, then the mass flow rate becomes independent of back pressure:

$$\dot{m} = AC_c\sqrt{2\rho\left(P_1 - P_v\right)} \tag{3}$$

This peculiar behavior is similar to compressible choking, in that the mass flow rate depends only on the upstream pressure, but not on downstream pressure. This behavior was observed by Randall in cavitating venturi nozzles [9]. It is still unknown whether this flow is actually sonic because of the complexity of the two-phase flow.

We can combine the definition of C_d, continuity, and Bernoulli's equation to obtain the following expression for the coefficient of discharge of a cavitating nozzle:

$$C_d = C_c\left(\frac{P_1 - P_v}{P_1 - P_2}\right)^{\frac{1}{2}} \tag{4}$$

The pressure ratio in the right side of Equation 4 turns out to be a very useful cavitation parameter and is referred to as K in the remainder of this paper.

$$K \equiv \frac{P_1 - P_v}{P_1 - P_2} \tag{5}$$

Nurick plotted the coefficient of discharge versus the cavitation parameter, K on log-log axes in order to verify the square root dependence of C_d on K [6]. He observed that the data from the cavitating region lay on a straight line with a slope of one-half, where C_c is the value of the Y-intercept. At some point, the value of K is high enough that the nozzle no longer cavitates. The higher values of K occur when the difference between the upstream and downstream pressure is small. At high values of K the coefficient of discharge stays fairly constant or decreases with increasing K and thus falls to the right of the cavitating line. This variation occurs because the coefficient of discharge is no longer a function of K, but depends on the Reynolds Number instead. In order to further validate Nurick's findings, we have collected more data for sharp nozzles with an L/D ratio of about 4. The data come from real-scale experiments as well as scaled-up experiments and spans sixty years of research [8, 10, 11, 12, 13]. As shown in Fig. 2, this wide variety of sources tends to confirm Nurick's hypothesis.

In an actual injector P_1 represents the sac pressure. Unfortunately, it is extremely difficult to measure the sac pressure of a working injector. Instead, fuel injectors may be equipped with a pressure transducer just *upstream* of the needle. Because the exact sac pressure is not known, we must contend with the fact that our measured coefficient of discharge will actually include strong needle effects. During periods of low needle lift there will most likely be a large pressure loss across the needle [14]. For the beginning and ending portions of the injection, the needle will dominate the behavior of the coefficient of discharge. Due to needle effects, the measured value of K is only credible during large needle lift. For this reason, the bulk of the previous analysis should be applied to the portion of injection where the needle is nearly fully open.

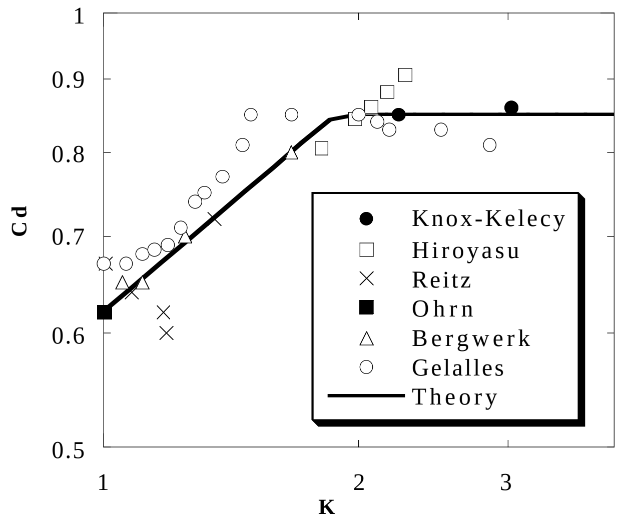

Figure 2. Experimental coefficient of discharge versus cavitation parameter

EXPERIMENTAL APPARATUS

The experimental apparatus includes: (1) a high pressure unit injector system for multi-hole injector experiments; (2) a low pressure pump line injection system for single-hole injector experiments. The details of these systems are described as follows.

Multi-hole Unit Injector System

To study the cavitation phenomena of transient Diesel sprays injected from a multi-hole tip, an experimental fuel injection system with a Bosch-type flow bench was used, as shown in Fig. 3.

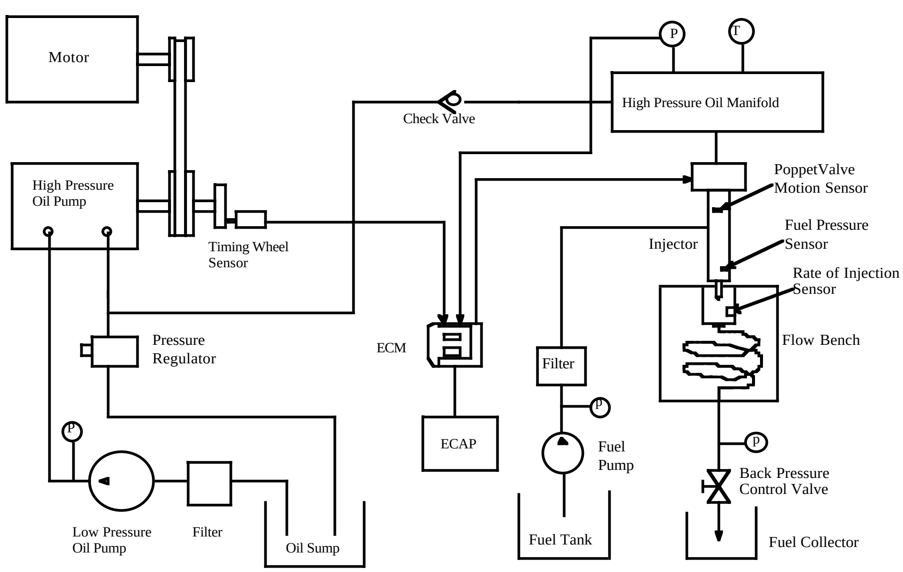

Figure 3. Diagram of multi-hole injector system and flow bench

The injection system consists of a hydraulic system, a fuel system, a control system, and an injector. The hydraulic system pressurizes the oil manifold to provide the injection energy. The fuel used for this experiment was Diesel No.2 fuel with a density of 0.8515 g/cm^3 at 25°C, and a viscosity of 2.82 cs at 40°C. The control system consists of sensors, an electronic control module (ECM), and an electronic control analyzer programmer (ECAP). The injector is a hydraulic electronic unit injector which consists of three main components: a control valve, an intensifier plunger and barrel, and a nozzle. The valve is an electronically controlled solenoid-poppet valve whose purpose is to start and stop the injection process. For more detailed information on this injector and other components see Stockner et al. [15].

Two injector tips were used, one with sharp holes and the other with rounded-inlet holes. The injector nozzles are mini-sac type, multi-hole Diesel nozzles, and have six holes with a sac volume about 0.41 mm^3. The nozzle holes for the sharp-edged tip have a 0.243 mm hole diameter. The rounded-nozzle hole diameters are 0.259 mm. The exact radii of curvature of the nozzle inlets have not been measured. Both nozzle tips have a 140° injection angle and a hole length of 0.755 mm. The *L/D* ratio is 3.107 for the sharp nozzles and 2.92 for the rounded nozzles. The injector is instrumented with a solenoid-poppet valve motion sensor and a fuel injection pressure sensor. The poppet valve motion sensor detects the lift of the solenoid-poppet valve which corresponds to the needle-lift movement. The fuel injection pressure signal is picked up by a strain gauge which is located upstream of the nozzle check valve.

The Bosch-type of flow bench is set up for controlling the back pressure and collecting the fuel mass. The principle behind the meter relates the injection rate to the pressure wave produced by the injection [16]. The flow bench has a piezoelectric transducer mounted close to the injector exit, which picks up the injection flow rate signal. Following the injector exit is a 23 m length of 6.35 mm ID tin-plated steel tubing. The pressure relief valve is located at the end of the tubing, which maintains the pressure downstream of the injector. The back pressure is monitored by a liquid filled, Bourdon tube pressure gauge with 3% accuracy.

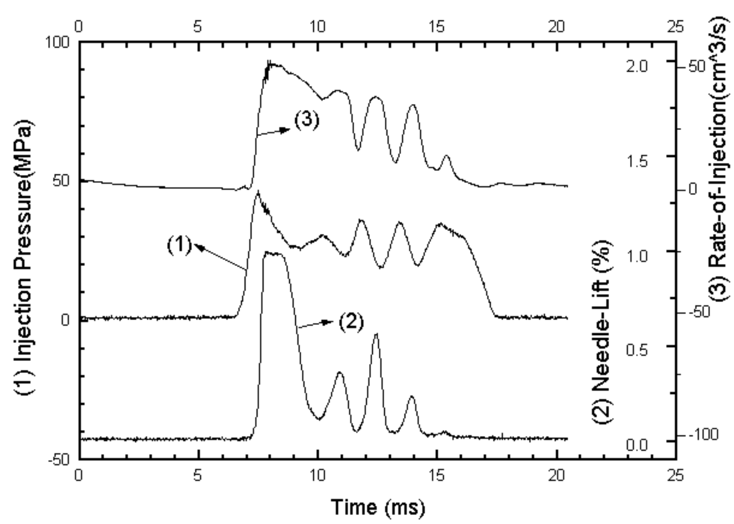

Figure 4. Data from the multi-hole injector, sharp-inlet tip

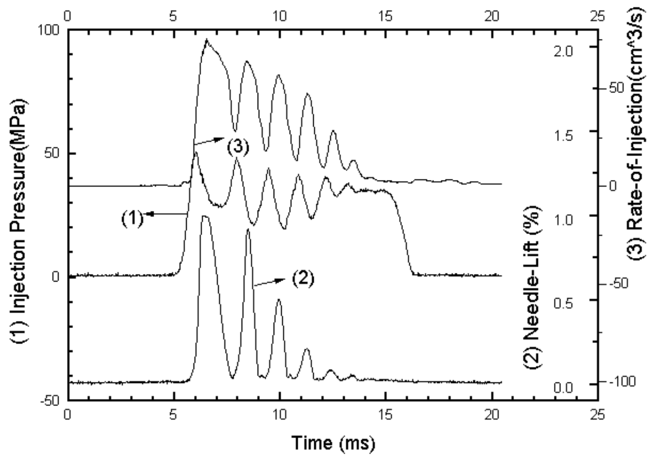

Figure 5. Data from the multi-hole injector, rounded-inlet tip

The experiments were run by keeping the injection pressure peak at 46 MPa, and varying the back pressure in the range of 0 to 27 MPa gage pressure. To determine the injection rate for each case, the injected mass was collected over a certain time interval, and the rate of injection signal was recorded based on time averaging. The rate-of-injection, fuel injection pressure trace, and the poppet valve movement signals, which were recorded using a Tektronix digital storage oscilloscope, are shown in Fig. 4 and 5. More detailed information on the conversion of the raw signals will be given in the Results and Discussion section.

Pump-line Single Hole Injector System

In order to observe the behavior of a Diesel injector over a larger cavitation parameter range, another fuel injection system was also used. This injection system consisted of a DC Motor, a Bosch injection pump, two solenoid valves, a check valve, speed and injection controllers and an injector, as drawn in Fig. 6.

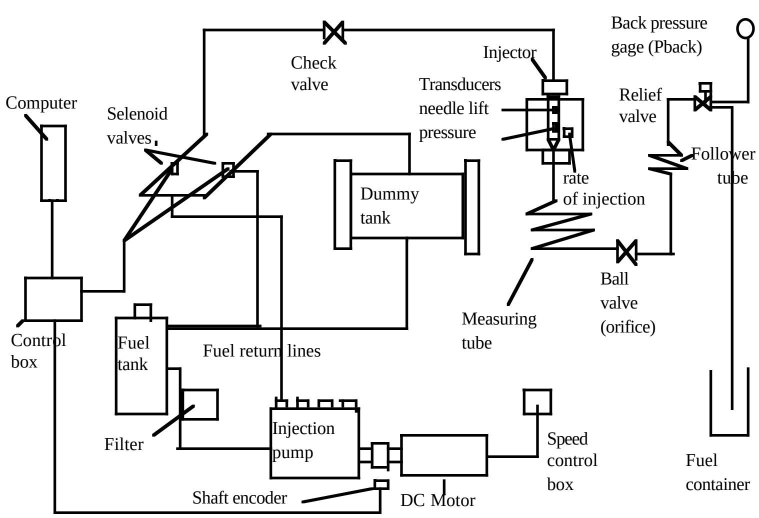

Figure 6. Pump line single hole injector system

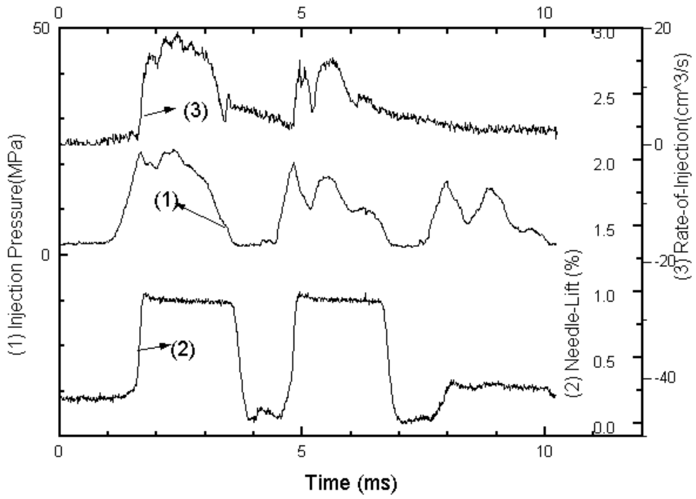

Figure 7. Data from the single hole injector

The Bosch-type flow bench used with this injector is slightly different than the one used with the unit injector system. The measuring tube used in this Bosch bench has a diameter of 4.90 mm ID, and a length of 24.4 m. The injector shield located on the bench has four strain gages on its inside wall for measuring the rate of injection. The back pressure in the measuring tube is precisely controlled in a range of 0-13 MPa by using a relief valve. In order to reduce the effect of reflection waves in the measuring tube, two solenoid valves controlled by a personal computer were used. By injecting into a dummy tank, the pause between injections in the Bosch meter was long enough for the reflection waves to dissipate.

The jerk type injection pump and single-hole injector enabled us to operate at injection pressures of 13-26 MPa, considerably lower than the minimum injection pressure for the multi-hole injector. The injector is instrumented with an injection pressure transducer and needle lift proximator. The pressure transducer is a strain gage located close to the sac volume, upstream the injector needle. A sac type single hole nozzle with an orifice diameter of 0.406 mm and a length of .8 mm was used for low pressure injection experiments. Data from this apparatus is shown below in Fig. 7.

RESULTS AND DISCUSSION

To analyze the data taken from the multi-hole injector instrumentation and the flow bench, voltages were collected from 256 injections. There was very little cycle-to-cycle variation observed in the signals, so the average of these 256 injections was used. The amount of fuel injected was collected over a measured time interval and the mass per injection was calculated. Then, the signal from the rate of injection piezoelectric pressure transducer was integrated and normalized to give the correct injected mass. The coefficient of discharge, as given by Eqn. 2, for the multi-hole tips is shown below in Fig. 8.

Although the curves of Fig. 4 and 5 clearly show the needle position oscillating, along with the rate of injection and the upstream pressure, the effect on the coefficient of discharge is not obvious. Since the needle was not seated, it may have a time-varying effect on the coefficient of discharge. Because of possible

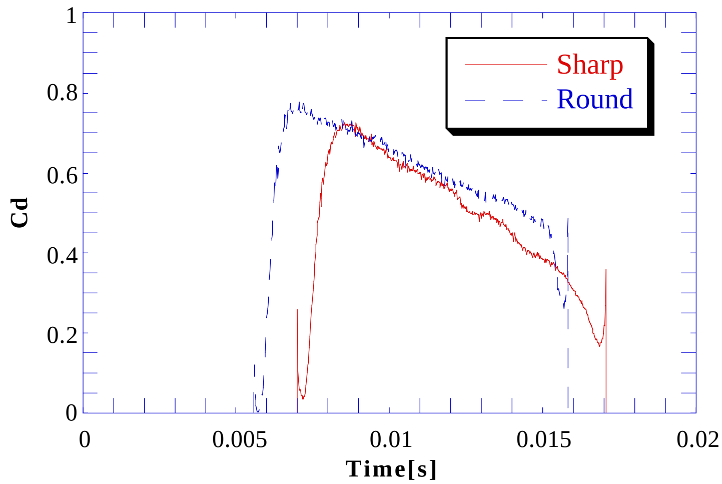

Figure 8. Coefficient of discharge for the multi-hole tips at a back pressure of 14.4 MPa

errors due to needle effects, only data points with a needle lift of greater than 98% were used for our analysis.

The experiments were run by keeping all the important parameters constant while varying back pressure. In order to combine the results of various runs into a single curve, we divided the *K* range into several small "bins." Each data point was put into one of these bins and the coefficients of discharge were averaged. This allowed the construction of a curve that incorporated a large number of instantaneous data points from each run. The measurements of the coefficient of discharge of the multi-hole injector with varying cavitation parameter are shown on a log-log plot in Fig. 9. The theoretical line drawn with the points is for a slope of one-half, with a *Y*-intercept of 0.49.

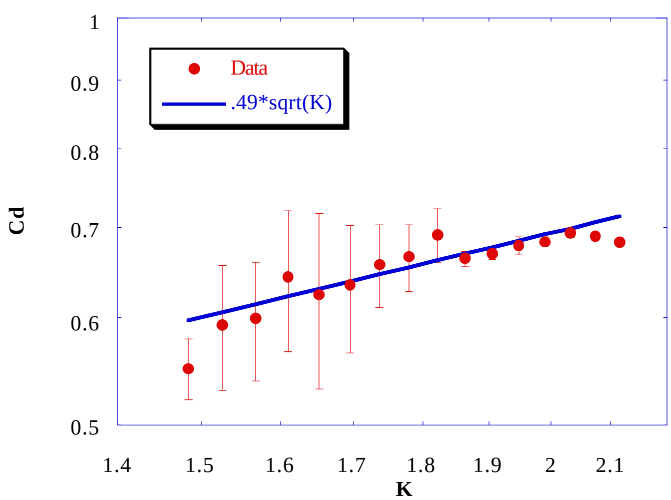

Figure 9. Coefficient of discharge for the multi-hole injector, sharp nozzle inlets. Error bars show plus and minus one standard deviation.

Due possibly to losses from the flow through the injector mechanism, the measurements of coefficient of discharge are about twenty percent lower than the predictions for a simple orifice. These losses do not vary with back pressure and thus do not change the slope of the curve, but rather reduce the *Y*-intercept from the theoretical value of 0.611 to 0.49. The strong resemblance of the measurements of coefficient of discharge in the sharp, multi-hole tip to the curve shown in Fig. 2 suggests that the nozzles are cavitating. The data taken from the sharp nozzles also show the characteristic slope of one-half predicted by the one-dimensional model. If some of the nozzles were cavitating and others were non-cavitating, we would expect the slope of this line to lie somewhere between one-half and zero. However, it appears from the data of Fig. 9 that most or all of the orifices are cavitating.

The data taken with rounded nozzles varies little with increasing K and behaves more like a non-cavitating nozzle. The results from the rounded-inlet, multi-hole tip are shown in Fig. 10 along with a correlation for non-cavitating nozzles [17]. The data from the rounded nozzle do not show the characteristic behavior indicative of cavitation. Instead, the coefficient of discharge remains fairly level at varying values of the cavitation parameter, consistent with the behavior of a non-cavitating nozzle.

The results with the single-hole injector were slightly different. The injection pressures tended to be much lower than in the multi-hole injector, which enabled us to achieve a wider range of *K*. Unfortunately, the pump line system tended to exhibit much more cycle-to-cycle variation which prevented us from taking an average over multiple injections. Because the data from the single-hole injector was taken for single injections, the noise level tended to be high.

Since the bench was fitted with a strain gage on the measuring tube for measuring rate of injection, we could analyze the data using a different method. We could convert the strain gage signal directly to an instantaneous pressure measurement, and use the one-dimensional hydraulic pulse relation originally intended by Bosch [16]. This relation gives the volume flow rate, *Q*, as a function of the measuring tube interior cross sectional area, *A*, the sound speed of the fluid, *a*, the density, ρ and the pressure pulse strength, *dp*.

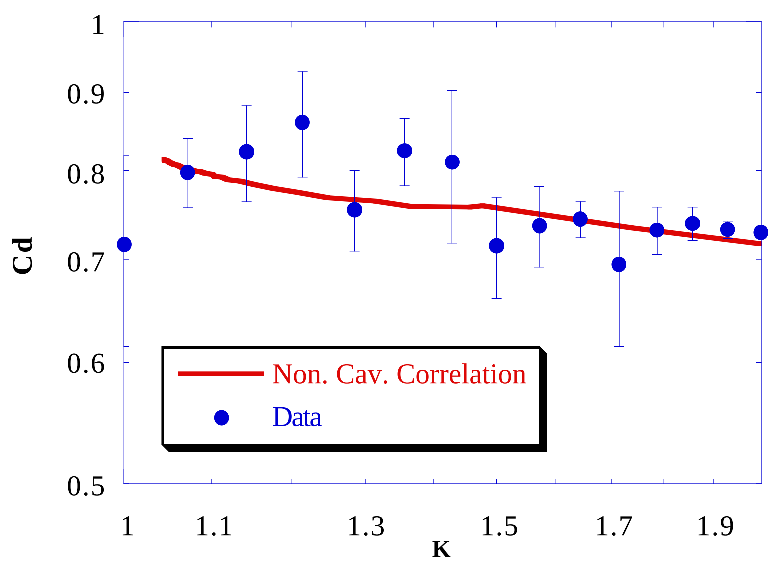

Figure 10. Coefficient of discharge for the multi-hole injector, rounded nozzle inlets. Error bars show plus and minus one standard deviation.

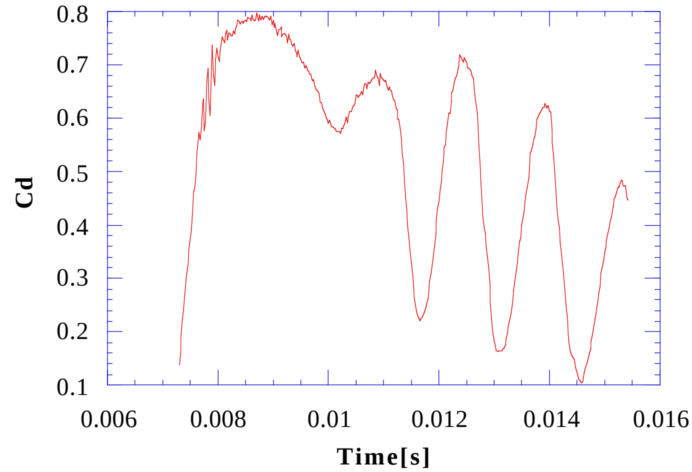

Figure 11. Coefficient of discharge for the single-hole nozzle with a back pressure of 4.1 MPa

$$Q = \frac{A}{a \cdot \rho} dP \qquad \{6\}$$

Bower has shown that this method gives the same results as the integration method used for the multi-hole injector, within 2% [18]. Since the hydraulic pulse method requires the speed of sound through the fuel, we measured the time required for an injection pulse to travel down the measuring tube and back to the transducer. We found the speed of sound at a moderate back pressure to be about 1515 m/s. The resultant coefficient of discharge from a typical injection is shown in Fig. 11. The curve has several peaks, which may be a result of the needle moving up and down.

The conversion from pressure and flow rate values to a C_d versus K curve was the same as for the multi-hole injectors. The measurements from the single-hole nozzle are plotted in Fig. 12.

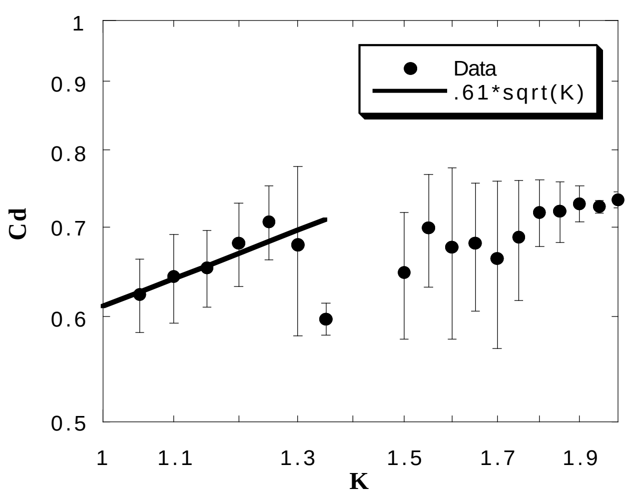

Figure 12. Coefficient of discharge for the single hole injector. Error bars show plus and minus one standard deviation.

We would also expect that at values of K above 2 the data should begin to fall below the cavitating line, as seen in Fig. 2. Due to the limits on the back pressure and the injection pressure of the multi-hole injector, we were not able to achieve high enough values of K to clearly demonstrate this trend in the multi-hole tips. However, some deviation below the cavitation line can be seen in Fig. 12 at K greater than 1.5, with data taken from the single-hole injector. The data taken from the single-hole injector injector falls near the line predicted by the one-dimensional cavitation theory for K less than 1.4.

CONCLUSIONS

The coefficient of discharge has been measured in two different types of injectors under transient conditions. Measurements were made with in a single-hole sharp-inlet tip; a multi-hole, sharp-inlet tip; and a multi-hole, rounded-inlet tip. The behavior of the coefficient of discharge with varying values of a cavitation parameter was compared to experimental data and to the predictions of a one-dimensional theory. For a sharp-inlet, multi-hole tip, the behavior was consistent with cavitation. The characteristic square-root dependence on K was identified, as predicted by theory. For the same injector, but with a rounded-inlet tip, the behavior of the coefficient of discharge resembled that of a non-cavitating nozzle. In a single-hole injector a qualitative behavior similar to a cavitating nozzle and the characteristic square-root dependence was noted.

This measurement technique is applicable to a variety of actual fuel injectors, not just scaled-up models. It allows for the fact that the nozzle geometry is not precisely known, due to manufacturing limitations and normal wear. It requires instrumentation which does not significantly change the behavior of the injector, as well as a Bosch flow bench capable of operating at high back pressures.

ACKNOWLEDGEMENTS

We would like to acknowledge the financial support of the Army Research Office under Grant No. DAAH04-94-G-0328 and the technical assistance of Lucas Diesel Systems, and Caterpillar Inc.

REFERENCES

1. T. F. Su, P. V. Farrell, and R. T. Nagarajan, "Nozzle Effects on High Pressure Diesel Injection," SAE Paper No. 950083, 1995.

2. Celia Soteriou, Richard Andrews, and Mark Smith, "Direct Injection Diesel Sprays and the Effect of Cavitation and Hydraulic Flip on Atomization," SAE Paper No. 950080, 1995.

3. H. Chaves, M. Knapp, A. Kubitzek, F. Obermeier, and T. Schneider, "Experimental Study of Cavitation in the Nozzle Hole of Diesel Injectors Using Transparent Nozzles," SAE Paper No. 950290, 1995.

4. W. Bergwerk, "Flow Pattern in Diesel Nozzle Spray Holes," *Proceedings of the Institute of Mechanical Engineers*, vol. 173, 1959.

5. R. von Mises, "Berechnung von Ausfluss und Ueberfallzahlen," *Zeitschrift des Vereins deutscher Ingenieure*, vol. 61,1917.

6. W. H. Nurick, "Orifice Cavitation and Its Effects on Spray Mixing," *Journal of Fluids*

Engineering, vol. 98, 1976.

7. F. Numachi, M. Yamabe, and R. Oba, “Cavitation Effect on the Discharge Coefficient of the Sharp-Edged Orifice Plate,” *Journal of Basic Engineering*, March, 1960.

8. H. Hiroyasu, M. Arai, and M. Shimizu, “Break-Up Length of a Liquid Jet and Internal Flow in a Nozzle,” *ICLASS-91* Gaithersburg, MD, July 1991.

9. L. N. Randall, “Rocket Applications of the Cavitating Venturi,” *ARS Journal*, Jan-Feb, 1952.

10. Andrea L. Knox-Kelecy and Patrick V. Farrell, “Internal Flow in a Scale Model of a Diesel Fuel Injector Nozzle,” SAE Paper No. 922308, 1992.

11. Rolf Deneys Reitz, *Atomization and Other Breakup Regimes of a Liquid Jet*, Ph.D. thesis, Princeton Univ., 1978.

12. T. R. Ohrn, D. W. Senser, and A. H. Lefebvre, “Geometric Effects on Spray Cone Angle for Plain-Orifice Atomizers,” *Atomization and Sprays*, vol. 1, 1991.

13. A. G. Gelalles, “Coefficients of Discharge of Fuel Injection Nozzles for Compression-Ignition Engines,” NACA Technical Memo. 373, 1931.

14. Horst Hardenberg, “Die Nadelhubabhaengigkeit der Durchflussbeiwerte von Lochduesen fuer Direkteinspritz-dieselmotoren,” *Motortechnische Zeitschrift* vol. 46, 1985.

15. A. R. Stockner, M. A. Flinn, and F. A. Camplin, “Development of the HEUI Fuel System-Integration of Design, Simulation, Test, and Manufacturing,” SAE Paper No. 930271, 1993.

16. W. Bosch, “The Fuel Rate Indicator: A New Measuring Instrument for Display of the Characteristics of Individual Injection”, SAE Paper No. 660749, 1966.

17. A. Lichtarowicz, R. K. Duggins, and E. Markland, “Discharge Coefficients for Incompressible Non-Cavitating Flow Through Long Orifices,” *Journal of Mechanical Engineering Science* 7(2), 1965.

18. Glenn R. Bower and David E. Foster, “A Comparison of the Bosch and Zuech Rate of Injection Meters,” SAE Paper No. 910724, 1991.